



# Differentiating Diffusivity in Different Channels of ZSM-5 Zeolite by Pulsed Field Gradient (PFG) NMR

Shu Zeng,<sup>[a, b]</sup> Shutao Xu,<sup>\*[a]</sup> Shushu Gao,<sup>[a, b]</sup> Mingbin Gao,<sup>[a, b]</sup> Wenna Zhang,<sup>[a]</sup> Yingxu Wei,<sup>\*[a]</sup> and Zhongmin Liu<sup>\*[a, c]</sup>

Differentiating the diffusivity in straight channel and sinusoidal channel of ZSM-5 zeolite is a prerequisite for catalyst optimization for the required product distribution with specific orientation. Herein, the intracrystalline diffusivities of n-butane and iso-butane in power ZSM-5 zeolite were investigated by pulse field gradient (PFG) NMR, respectively. Different diffusion behaviors of the selected isomers were revealed. The effective self-diffusion coefficient of n-butane is about three orders of magnitude higher than that of iso-butane. For the selected isomers, the opposite loading-dependence were presented in self-diffusion coefficients. Moreover, an equation containing diffusion tensors in different directions in orthogonal coordinate was successfully applied to fit the diffusion coefficients of n-butane in straight and sinusoidal channel of ZSM-5, respectively. The diffusivity of n-butane in straight channel is nearly one order of magnitude faster than that in sinusoidal channel, predicting its dominant diffusion path.

ZSM-5 zeolite is a typical representative of shape-selective catalyst and widely used in catalytic reaction, such as methanol-to-propylene (MTP) reaction, isomerization, alkylation and aromatization.<sup>[1–3]</sup> The shape-selectivity is closely related to the diffusion anisotropy of guest molecules in the host zeolites, when pore size is comparable to the kinetic diameter of guest molecules.<sup>[4]</sup> Importantly, the diffusion anisotropy is mainly dependent on pore structure. ZSM-5 zeolites with MFI topology,

consisting of a sinusoidal channel (5.1×5.5 Å) in the a–c plane and a straight channel (5.3×5.6 Å) in the b direction, provide two types of confined spaces. It is indicated that the sinusoidal channel limits the diffusion of large aromatic molecules in methanol-to-hydrocarbons (MTH) process, and the selectivity of products can be manipulated by adjusting the proportion of two channels.<sup>[5]</sup> The lower length ratio of the b/a axes of the ZSM-5 crystal, the higher selectivity of the aromatics.<sup>[6]</sup> Ryong et al. synthesized single-unit-cell ZSM-5 nanosheet with 2 nm thick along the b-axis, which extremely shortens the diffusion path of reactants and products, as well as dramatically suppresses coke deposition during methanol-to-gasoline conversion.<sup>[7]</sup> Therefore, knowledge of the mass transport in straight and sinusoidal channels can contribute to the understanding of product distribution in the catalytic reaction and the guidance of catalyst synthesis with specific orientation.

The diffusion anisotropy in ZSM-5 has been studied by theoretical and experimental methods, such as molecular dynamics (MD) simulations,<sup>[8]</sup> quasi-elastic neutron scattering (QENS),<sup>[9,10]</sup> infra-red micro-imaging,<sup>[11,12]</sup> interference microscopy,<sup>[13,14]</sup> frequency response (FR) technique,<sup>[15]</sup> pulsed field gradient (PFG) nuclear magnetic resonance (NMR) method<sup>[16–19]</sup> and so on. Pulsed field gradient (PFG) NMR spectroscopy, as a non-invasive method, can be used to study the molecular migration with respect to the coordinate of the applied field gradient, revealing the vital role played by pore structure of ZSM-5 zeolite. After summarizing the PFG NMR work in the last decades, generally, there are three different approaches to determine the diffusion anisotropy of zeolite: (1) by intuitively analyzing the shape of the NMR signal attenuation with increased field gradient strength in powder sample,<sup>[16]</sup> (2) by changing the direction of the magnetic field gradient,<sup>[17]</sup> (3) by using an oriented crystallites,<sup>[18]</sup> or a single crystal.<sup>[19]</sup> The second method is limited by the NMR hardware. The third method is limited by sample preparation which requires an effective orientation of crystallites or a sufficiently large single crystals even up to millimeter scale.

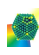
It is worth mentioning that Kärger and his coworkers<sup>[16–21]</sup> have obtained numerous important results in studying diffusion anisotropy of zeolite, especially for ZSM-5 using PFG NMR. The ratio of the diffusion coefficient of methane molecules in every coordinate direction in the orthogonal coordinate system was determined for the large single ZSM-5 crystal. Furthermore, differentiating the diffusivities of methane molecules in orthogonal coordinates of crystals combining with the molecular dynamics (MD) simulations were performed.<sup>[16,18]</sup> However,

[a] S. Zeng, Prof. S. Xu, S. Gao, M. Gao, Dr. W. Zhang, Prof. Y. Wei, Prof. Z. Liu  
National Engineering Laboratory for Methanol to Olefins  
Dalian National Laboratory for Clean Energy  
iChEM (Collaborative Innovation Center of Chemistry for Energy Materials)  
Dalian Institute of Chemical Physics  
Chinese Academy of Sciences  
Dalian 116023 (P. R. China)  
E-mail: xushutao@dicp.ac.cn  
weiyx@dicp.ac.cn  
liuzm@dicp.ac.cn

[b] S. Zeng, S. Gao, M. Gao  
University of Chinese Academy of Sciences  
Beijing 100049 (P. R. China)

[c] Prof. Z. Liu  
State Key Laboratory of Catalysis  
Dalian Institute of Chemical Physics  
Chinese Academy of Sciences  
Dalian 116023 (P. R. China)

 Supporting information for this article is available on the WWW under <https://doi.org/10.1002/cctc.201901689>

 This publication is part of a Special Collection on "Advanced Microscopy and Spectroscopy for Catalysis". Please check the ChemCatChem homepage for more articles in the collection.

differentiating diffusivities in different channels of MFI structure for long chain alkane with lower mobility is still a challenge.

In this work, n-butane and iso-butane, isomers of C4 alkane, were selected as guest molecules to study the diffusion anisotropy in ZSM-5 zeolite. Different diffusion behaviors of n-butane and iso-butane in ZSM-5 zeolite were revealed, respectively. With assigning the diffusion along y axis to the motion in straight channel direction and the diffusion along x axis to the motion in sinusoidal channel direction of ZSM-5 crystal, respectively, the diffusivities of n-butane in two channels were differentiated by analyzing and fitting the shape of the spin-echo attenuation curve.

For powder sample, there are various orientations of the crystals with respect to the applied field gradient direction. The self-diffusion coefficient derived from the echo attenuation is a weighted average of the diffusion coefficients along the principal axes. Therefore, the diffusivity can be described as a tensor rather than a single diffusion coefficient, and the information about the diffusion tensor is contained in the shape of the spin echo attenuation, which follows the Equations (1) and (2).<sup>[22–23]</sup>

$$\Psi(C, \vartheta, \phi) = \frac{1}{4\pi} \int_{-1}^1 \exp \{ -C(D_{zz} \cos^2 \vartheta + D_{yy} \sin^2 \vartheta) \} I(\vartheta) d(\cos \vartheta) \quad (1)$$

$$I(\vartheta) = \int_0^{2\pi} \exp \{ -C \sin^2 \vartheta (D_{xx} - D_{yy}) \cos^2 \phi \} d\phi \quad (2)$$

In the above formulas,  $\Psi(C, \vartheta, \phi)$  is the ratio of the signal amplitudes with and without gradient field, respectively, C presents the  $(\gamma \delta g)^2 (\Delta - \delta/3)$ ,  $D_{xx}$ ,  $D_{yy}$  and  $D_{zz}$  denote the principal elements of the diffusion tensor,  $\vartheta$  and  $\phi$  are the orientation of the applied field gradient with respect to the principal axes system,  $\gamma$  stands for the gyromagnetic ratio of the nuclei,  $g$  is the gradient strength,  $\delta$  is the gradient duration, and  $\Delta$  is the diffusion time. For the isotropic system, the self-diffusion coefficients of three orthogonal directions are equal, that is  $D_{xx} = D_{yy} = D_{zz}$ . Equation (1) can be transferred into Equation (3)  $D_{\text{eff}}$  represents the effective diffusion coefficient.

$$\langle \Psi(C) \rangle = \exp \{ -\gamma^2 \delta^2 g^2 D_{\text{eff}} (\Delta - \delta/3) \} \quad (3)$$

According to the well-known Einstein's equation 4, the diffusion coefficient is related to the molecule mean square displacement and diffusion time  $\Delta$ . As for a sufficiently large crystal, diffusion which is slow enough and short observation times, molecular propagation inside the crystals remains essentially not disturbed by the crystal boundary and the intercrystalline space [Eq. (4)].<sup>[24]</sup>

$$\langle r(t)^2 \rangle = 6D_{\text{eff}} \Delta \quad (4)$$

ZSM-5 (Si/Al = 61.3, measured by ICP) used in this work was H-type and obtained by ion exchange from Na-ZSM-5 according to Ref 25.<sup>[25]</sup> The crystal size of the prismatic zeolite is approximately  $30 \times 30 \times 80 \mu\text{m}^3$  as shown in the Figure S1 and

S2 (seen in ES†). The synthesized ZSM-5 zeolite only has micropores according to the  $\text{N}_2$  absorption–desorption experiment (Figure S3 in ES†). The framework Si/Al of 61.9 determined by the  $^{29}\text{Si}$  MAS NMR, is slightly higher than the result of ICP (Figure S4 in ES†).  $^{27}\text{Al}$  MAS NMR spectrum shows four-coordinated alumina as the main in H-ZSM-5 (see in ES†, Figure S5). After loading with a certain amount of n-butane and iso-butane, respectively, the chemical shifts of adsorbed n-butane and iso-butane are both 2.7 ppm as shown in Figure 1a and Figure 1b. The semi-logarithmic plots of  $^1\text{H}$  PFG NMR echo attenuation curve are presented in Figure 1c and Figure 1d. It is noticed obviously that the measured PFG NMR spin-echo attenuation curve of iso-butane follows a linear relationship between  $\ln \Psi$  and C or a single-exponential behavior between  $\Psi$  and C. However, the spin-echo attenuation curve of n-butane distinctly deviates from the linear relationship (Figure 1d), which indicates that the measured attenuation curve contained more than one kind of intracrystalline diffusivities. It was reported by Furukawa and Fernandez in the ZSM-5 zeolite, in which the n-butane molecules can stay in both the straight and sinusoidal channels of the ZSM-5, while the iso-butane molecules are inclined to locate at the intersection of the channels according to the Configurational-Bias Monte Carlo (CBMC) simulations.<sup>[26,27]</sup> It can be guessed that the preferred location of the molecules may affect the relation between the diffusion tensor elements, and give rise to different type of spin-echo attenuation curve. Based on the above theoretical simulation results, therefore, in the case of anisotropic diffusion of n-butane in ZSM-5, the first five points of the attenuation curve were used to acquire an effective diffusivity ( $D_{\text{eff}}$ ).<sup>[27]</sup> The intracrystalline diffusivity of iso-butane was obtained through Eq. (3).

As seen in ES† (Table S1), the effective self-diffusion coefficients for iso-butane and n-butane were determined with the temperature varying from 303 to 333 K under different concentrations, respectively. The effective self-diffusion coefficients ( $D_{\text{eff}}$ ) of  $10^{-13} \text{ m}^2/\text{s}$  order of magnitude for iso-butane and  $10^{-10} \text{ m}^2/\text{s}$  order of magnitude for n-butane are presented. Compared to other's work, Banas<sup>[28]</sup> reported a value of  $2 \times 10^{-12} \text{ m}^2/\text{s}$  for iso-butane in MFI using PFG NMR at 363 K. Fernandez<sup>[27]</sup> utilized the MAS PFG NMR to obtain the effective diffusivities of iso-butane and n-butane are  $1.63 \times 10^{-12} \text{ m}^2/\text{s}$  and  $3.55 \times 10^{-10} \text{ m}^2/\text{s}$  at 300 K, respectively. Therefore, the values of  $3.10 \times 10^{-13} \text{ m}^2/\text{s}$  for iso-butane and  $3.36 \times 10^{-10} \text{ m}^2/\text{s}$  for n-butane at 303 K in present work are reasonable. Furthermore, loading-dependent experiments of n-butane and iso-butane were also performed. The loading dependence of the diffusion coefficient is related to the pore properties of zeolite, such as pore size, pore shape and pore type, and multiple loading-dependent diffusivities have been studied in the previous work.<sup>[29,30]</sup> A general comparison indicates that the diffusion coefficient of n-butane is three orders of magnitude higher than that of iso-butane, which is mainly due to the strong steric hindrance of iso-butane. The opposite variation tendency of loading-dependent self-diffusion coefficients of the selected n-butane and iso-butane were presented, as shown in Figure 2. This is probably due to the different adsorption

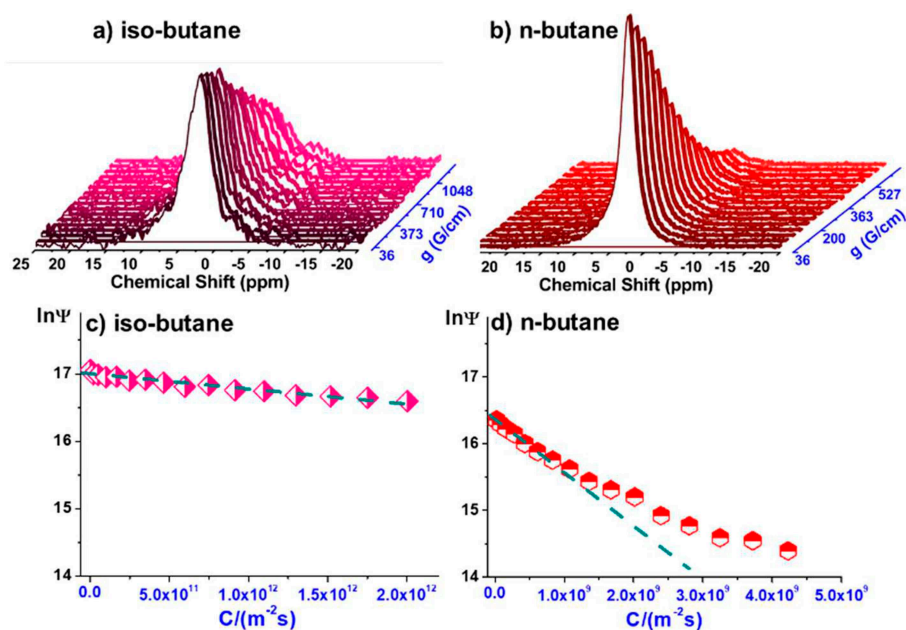


**Figure 1.** <sup>1</sup>H NMR spectra varying with gradient field strength of (a) iso-butane; (b) n-butane and semi-logarithmic plot of <sup>1</sup>H PFG NMR echo attenuation curves measured for (c) iso-butane; (d) n-butane in ZSM-5 zeolite at 333 K. The concentration is 4 molecules per unit cell. The dashed line is just for guidance. C denotes  $[(\gamma\delta g)^2(\Delta - \delta/3)]$ .

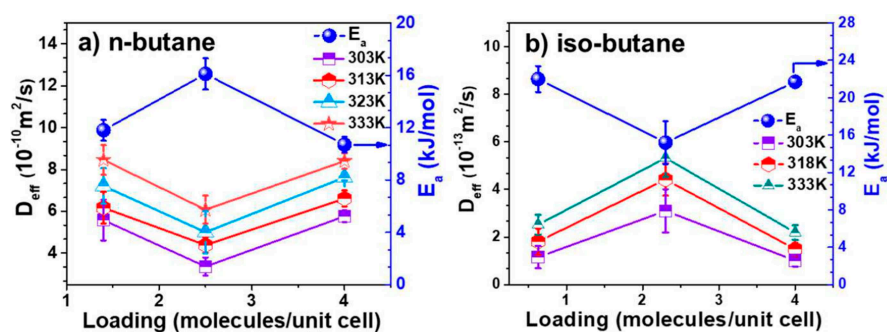


**Figure 2.** Effective self-diffusion coefficient and activation energy of (a) n-butane; (b) iso-butane vary with loading.

sites,<sup>[26]</sup> strength of the adsorbate-adsorbate interaction and the degree of confinement of the two molecules in ZSM-5 zeolite.<sup>[29,31]</sup> It was proved by Monte Carlo simulation that iso-butane only occupies the intersection channels of ZSM-5 when the loading is under 4 molecules per unit cell.<sup>[32]</sup> Therefore, the intersections of sinusoidal and straight channels are fully occupied at a loading of 4 molecules per unit cell, iso-butane must to seek residence in the other adsorption sites, which demands higher driving force and more energy. It can be speculated that the different adsorption site of iso-butane makes the variation tendency of diffusion coefficient differing from n-butane. Variable-temperature of self-diffusion were also performed, as shown in Figure 2. Effective self-diffusion coefficient increases as the temperature increases due to that diffusion is an active process. The apparent activation energy represents the energetic barrier that the guest molecule needs to overcome on diffusion pathways within molecular sieves.<sup>[33]</sup>

The apparent diffusion activation energy of iso-butane of 21.7 kJ/mol is higher than that of n-butane of 10.7 kJ/mol with the loading of 4 molecules per unit cell, respectively, which indicates that iso-butane molecule needs to overcome larger barrier than that of n-butane. With the increase of loading, the variation tendency of the apparent activation energy is opposite to that of self-diffusion coefficient of both n-butane and iso-butane. For diffusion activation energy concern, the tendency of loading-dependent is reasonable.

Based on the above analysis, although the self-diffusion varies with the loading and temperature, the diffusion of n-butane is obviously faster than iso-butane in the ZSM-5, which is closely correlated with molecular dimension and conformation. This role played by molecular dimension and shape in diffusion is further reflected by diffusion anisotropy in the MFI structure. As mentioned above, the notable deviation from a single-exponential behavior of n-butane in PFG NMR is

displayed due to the diffusion anisotropy in the MFI structure (Figure 1d). Given this consideration, to disclose such diffusion anisotropy in ZSM-5 zeolite, the diffusion in straight channel and sinusoidal channel of ZSM-5 was differentiated, respectively. According to the channel description, the directions of the x and y axes were marked to the sinusoidal and the straight channel, respectively. For the reason of absence of channel system directed along the z axis, the propagation of molecules in this direction is ascribed to proceeding in the alternating periods of migration along the segments of both channels.<sup>[34]</sup> The diffusion tensor of the directions follows the correlation rule [Eq. (5)].<sup>[34,35]</sup>

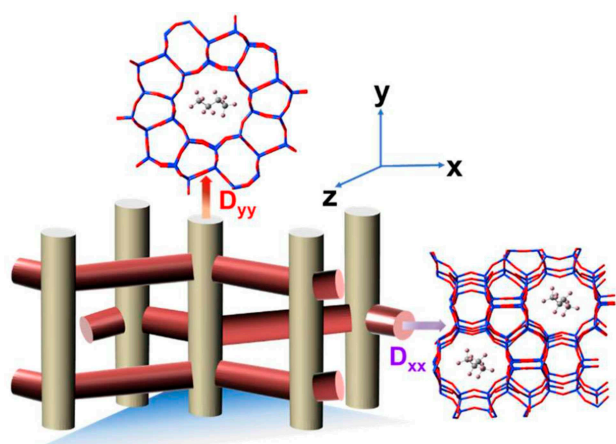
$$c^2/D_{zz}=a^2/D_{xx}+b^2/D_{yy} \quad (5)$$

where a, b, c denotes the unit cell lengths of ZSM-5 zeolite. By the very nature of the channel structure of ZSM-5 zeolite, mass transfer in z direction is much smaller in comparison with diffusion in x and y directions.<sup>[35,36]</sup> For the sake of simplicity, the diffusion tensor  $D_{zz}$  in Eq. (1) was approximated to zero under the studied situation, and the experimental data was fitted by Equations (6) and (2).

$$\Psi(C, \vartheta, \varphi) = \frac{1}{4\pi} \int_{-1}^1 \exp\{-CD_{yy}\sin^2\vartheta\} I(\vartheta) d(\cos\vartheta) \quad (6)$$

In the Eq. (6),  $D_{yy}$  was assigned to the diffusion along straight channel, also  $D_{xx}$  was assigned to the diffusion along sinusoidal channel as shown in Scheme 1. Since the pronounced nonexponential behavior of spin-echo attenuation curve of n-butane can also be elucidated by supposing the existence of several fractions of adsorbate molecules in different adsorption space and having different diffusivities.<sup>[34,37]</sup> In this situation, the attenuation curve of n-butane might be presented as a sum of two parts of exponential terms just like long-range diffusion [Eq. (7)].

$$\langle \Psi(C) \rangle = p \times \exp\{-CD_{yy}\} + (1-p) \times \exp\{-CD_{xx}\} \quad (7)$$



**Scheme 1.** Schematic view of the n-butane diffusing along straight channel and sinusoidal channel of ZSM-5 zeolite.

where p represents the probability of finding n-butane molecules in the straight channel.

In PFG NMR diffusion experiments, the diffusion time for iso-butane and n-butane is 200 ms and 10 ms, respectively. According to the Einstein's equation, the maximum root-mean-square displacement (RMSD) of iso-butane and n-butane is 0.8  $\mu\text{m}$  and 7.1  $\mu\text{m}$ , respectively, which are much smaller than the size of a single crystal ( $30 \times 30 \times 80 \mu\text{m}^3$ ). That means that the guest molecule remains in the intracrystalline space during the diffusion time of PFG NMR measurements and the measured diffusion coefficients are intracrystalline diffusivities. As presented in Figure S6, the observed spin-echo attenuation curves are well fitted by Eq. (6). Correspondingly, the diffusion coefficient of  $2.2 \times 10^{-9} \text{ m}^2/\text{s}$  and  $2.1 \times 10^{-10} \text{ m}^2/\text{s}$  for n-butane in the straight channel and sinusoidal channel are extracted with the loading of 4 molecules per unit cell at 333 K, respectively. Moreover, the diffusion coefficients of n-butane in straight channel and sinusoidal channel of ZSM-5 zeolite with different loadings at temperature varying from 303 to 333 K were determined by the same method, as shown in Figure 3. The diffusion coefficient of n-butane in straight channel of the  $10^{-9}$  order of magnitude and in sinusoidal channel of the  $10^{-10}$  order of magnitude were exhibited. A significant difference about one order of magnitude in self-diffusion coefficient of n-butane was displayed when molecule in straight channel and sinusoidal channel of ZSM-5 zeolite. This value is slightly larger than early works reported by Kärger,<sup>[35]</sup> in which a value of 5 times was estimated as an upper limit for the ratio between the diffusivities in x-y-z different crystal directions by theoretical calculation. It can be speculated that the longer alkane chain is, the greater difference of its diffusivities in different channels of ZSM-5 is. It is noteworthy from Figure 3d that the n-butane molecules almost have the same possibilities to be in the straight channel and sinusoidal channel, which successfully verified the theoretical results.<sup>[26,27,32]</sup> The ZSM-5 zeolite with short b-axis and fully opened straight channels synthesized by Wang<sup>[38]</sup> exhibited ultrahigh aromatic selectivity and longer lifetime, which may be ascribed to the faster transport of molecules in straight channels as indicated by the present work. This crystal-plane effect also is confirmed by the unilamellar MFI zeolite, in which the preferential formation of coke in external acid site rather than internal acid site compared with its conventional counterpart.<sup>[7]</sup>

Overall,  $^1\text{H}$  PFG NMR was used to study the intracrystalline diffusion coefficients of n-butane and iso-butane in large ZSM-5 crystal. A great difference in diffusion behaviour of n-butane and iso-butane in ZSM-5 zeolite was displayed, which implies more than one kind of intracrystalline diffusion modes of n-butane compared to iso-butane. The effective intracrystalline diffusion coefficient of n-butane is three orders of magnitude higher than that of iso-butane due to the molecular geometry. With assigning y axis to the direction of straight channel and the x axis to the direction of sinusoidal channel in ZSM-5 crystal according to the channel ascription in catalytic reaction, the diffusion of n-butane in these two channels were successfully differentiated by fitting the shape of the spin-echo attenuation curve directly. The diffusion coefficient in straight channel is



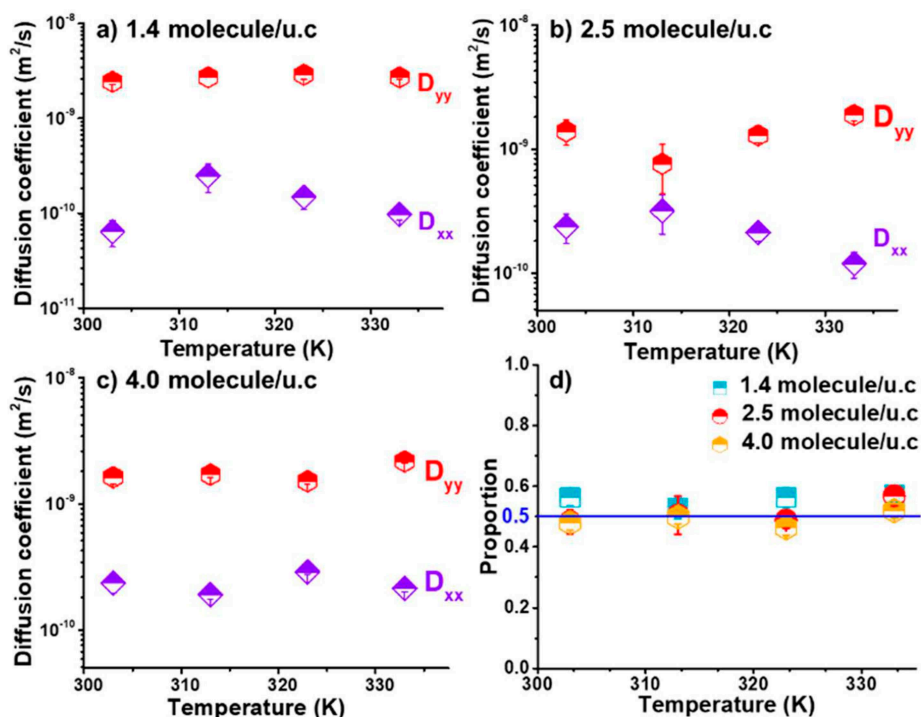


**Figure 3.** The diffusion coefficients of n-butane in straight channel and sinusoidal channel of ZSM-5 zeolite under different loadings with the temperature varying from 303 K to 333 K, respectively. (a) 1.4 molecule per unit cell; (b) 2.5 molecule per unit cell; (c) 4.0 molecule per unit cell; (d) the probability of finding n-butane molecules in the straight channel formats at different temperatures. The red semi-filled hexagon represents the diffusion coefficient of straight channels at the 10<sup>-9</sup> order of magnitude. The purple semi-filled rhombus represents the diffusion coefficients of sinusoidal channels at the 10<sup>-10</sup> order of magnitude.

almost an order of magnitude higher than that in sinusoidal channel. This method is of great importance in differentiating the predominant diffusion directions in complex catalyst channels, contributing to a better understanding of the mass transfer phenomena during the proceeding of catalytic reactions and providing a guidance for the catalyst synthesis with required specific orientation.

## Experimental Section

### Catalyst Synthesis

The large crystal ZSM-5 used in the diffusion experiments was synthesized according to reference 25 by the conventional hydrothermal method.<sup>[25]</sup> The gel was prepared by the following procedure. The mixture of silica sol (30%wt), tetrapropylammonium bromide (TPABr), sodium bicarbonate (NaHCO<sub>3</sub>), aluminum hydroxide (Al(OH)<sub>3</sub>) and distilled water was stirred at room temperature to form a homogenous gel. The standard composition of the reaction gel (as the formal molar oxides ratio) was 90 SiO<sub>2</sub>:1 Al<sub>2</sub>O<sub>3</sub>:1 Na<sub>2</sub>O:2100 H<sub>2</sub>O:9 TPABr. Then the gel was transferred to a stainless steel autoclave and crystallized at 183 °C for 5 days. After the crystallization, the solid products were obtained by centrifugation, washed with distilled water three times, and dried in air at 120 °C overnight. The sample was calcined at 923 K in air for 6 h to get rid of organic templates. The ZSM-5 zeolite was obtained by successive ion-exchange with 1 M NH<sub>4</sub>NO<sub>3</sub> solution at 353 K for three times. The solid to liquid ratio is 40, that means of

1 g catalyst corresponding to 40 ml NH<sub>4</sub>NO<sub>3</sub> solution. Finally, the as-synthesized was calcined at 873 K for 6 h in tube furnace.

### Characterization

The powder X-ray diffraction (XRD) patterns of as-synthesized ZSM-5 were recorded on a PANalytical X'Pert PRO X-ray diffractometer with Cu-K $\alpha$  radiation ( $\lambda = 1.54059 \text{ \AA}$ ) to determine the crystallinity and purity of zeolite. XRD patterns were recorded in the range of  $2\theta = 5\text{--}50^\circ$ , operating at 40 kV and 40 mA. The crystal morphology was observed by scanning electron microscopy (SEM) using a field emission SEM (Hitachi SU 8020). Nitrogen adsorption-desorption experiment was utilized to determine the BET surface area and micropore volume of the ZSM-5 zeolite as synthesized at 77 K (Micromeritics ASAP 2020). Before the measurement, zeolites were pretreated at temperature 673 K under vacuum. The specific surface area of the sample was calculated by BET equation, and the micropore area and volume were calculated by t-plot method. <sup>29</sup>Si NMR and <sup>27</sup>Al NMR experiments were performed on a Bruker Avance III 600 spectrometer equipped with 14.1T wide-bore magnet. The resonance frequencies in this field strength were 119.2 MHz and 156.4 MHz for <sup>29</sup>Si, <sup>27</sup>Al respectively. The <sup>29</sup>Si MAS NMR spectrum was recorded with a high-power proton decoupling sequence with a spinning rate of 8 kHz. The spinning rate of <sup>27</sup>Al spectra was 12 kHz. Chemical shifts of <sup>29</sup>Si spectra was referenced to kaolinite at -91.5 ppm, and that of <sup>27</sup>Al was referenced to Al (NO<sub>3</sub>)<sub>3</sub> solution at 0 ppm.

## Pulsed Field Gradient NMR Experiment

The intracrystalline diffusion coefficients of n-butane and isobutane in ZSM-5 zeolite were obtained from  $^1\text{H}$  PFG NMR experiments, which were carried out on a Bruker Avance III 600 spectrometer equipped with a Bruker diff50 diffusion probe and a maximum magnetic field gradient strength of 1800 G/cm in the z-direction. The basic principle of PFG NMR has been reported in detail elsewhere.<sup>[39,40]</sup> The stimulated spin-echo pulse sequence (13-interval sequence) was used to avoid the effects of internal magnetic field gradients in the porous materials.<sup>[41]</sup> The spin-echo attenuation could be obtained by linearly increasing a series of gradient strength  $g$  in 16 steps, while the gradient duration  $\delta$  and the diffusion time  $\Delta$  were kept constant. Additionally, temperature-dependent experiments were performed at 303, 313, 323 and 333 K for n-butane, 303, 318 and 333 K for iso-butane to obtain the apparent diffusion activation energies ( $E_a$ ), which can be calculated from the Arrhenius relationship

$$D = D_0 \exp\left(-\frac{E_a}{RT}\right)$$

Prior to  $^1\text{H}$  PFG NMR experiments, approximately 500 mg of ZSM-5 catalysts were pretreated at 693 K for 15 h under vacuum to completely remove adsorbed water and impurities in pore space. Subsequently, the catalysts after dehydration were transferred into an NMR glass tube with an outer diameter of 5 mm in argon glove box. The zeolite was loaded with a required amount of n-butane or iso-butane at room temperature using a home-built vacuum apparatus, then the glass tube was sealed off. All data were acquired under equilibrium conditions. The loadings of adsorbed molecules were calculated according to the ideal gas equation.

## Acknowledgements

This work was supported by the National Natural Science Foundation of China (21972142, 91745109, 21473182), LiaoNing Revitalization Talents Program (XLYC1807227), the Youth Innovation Promotion Association of the Chinese Academy of Sciences (2014165), the Key Research Program of Frontier Sciences, Chinese Academy of Sciences (QYZDY-SSW-JSC024), International Partnership Program of Chinese Academy of Sciences (121421KYSB20180007).

## Conflict of Interest

The authors declare no conflict of interest.

**Keywords:** PFG NMR · intracrystalline diffusion · ZSM-5 · straight channel · sinusoidal channel

- [4] L. Guedré, T. Binder, C. Chmelik, F. Hibbe, D. M. Ruthven, J. Kärger, *Materials*, **2012**, *5*, 721–740.
- [5] N. Wang, W. Sun, Y. Hou, *J. Catal.* **2018**, *360*, 89–96.
- [6] J. H. Yang, K. Gong, D. Y. Miao, F. Jiao, X. L. Pan, X. J. Meng, F. S. Xiao, X. H. Bao, *J. Energy Chem.* **2019**, *35*, 44–48.
- [7] C. Minkee, N. Kyungsu, K. Jeongnam, S. Yasuhiro, T. Osamu, R. Ryong, *Nature* **2009**, *461*, 246–249.
- [8] J. Kärger, P. Demontis, G. B. Suffritti, *J. Chem. Phys.* **1999**, *110*, 1163–1172.
- [9] H. Jobic, *Curr. Opin. Solid State Mater. Sci.* **2002**, *6*, 415.
- [10] H. Jobic, D. Theodorou, *Microporous Mesoporous Mater.* **2007**, *102*, 21.
- [11] C. Chmelik, L. Heinke, P. Kortunov, J. Li, D. Olson, D. Tzoulaki, J. Weitkamp, J. Kärger, *ChemPhysChem* **2009**, *10*, 2623.
- [12] L. Heinke, C. Chmelik, P. Kortunov, D. Ruthven, D. Shah, S. Vasenkov, J. Kärger, *Chem. Eng. Technol.* **2007**, *30*, 995–1002.
- [13] F. Hibbe, J. van Baten, R. Krishna, C. Chmelik, J. Weitkamp, J. Kärger, *Chem. Ing. Tech.* **2011**, *83*, 2211.
- [14] U. Schemmert, J. Kärger, J. Weitkamp, *Microporous Mesoporous Mater.* **1999**, *32*, 101.
- [15] L. Song, Z. L. Sun, L. H. Duan, J. Z. Gui, G. S. McDougall, *Microporous Mesoporous Mater.* **2007**, *104*, 115–128.
- [16] U. Hong, J. Kärger, H. Pfeifer, U. Müller, K. K. Unger, *Z. Phys. Chem.* **1991**, *173*, 225–234.
- [17] J. Kärger, D. M. Ruthven, *Diffusion in Zeolites and Other Microporous Solids*, Wiley, New York **1992**.
- [18] U. Hong, J. Kärger, R. Kramer, H. Pfeifer, G. Seiffert, *Zeolites* **1991**, *11*, 816–821.
- [19] N. K. Bär, J. Kärger, H. Pfeifer, *Microporous Mesoporous Mater.* **1998**, *22*, 289–295.
- [20] U. Hong, J. Kärger, H. Pfeifer, *Z. Phys. Chem.* **1991**, *173*, 225–234.
- [21] F. Stallmach, J. Kärger, C. Krause, M. Jeschke, U. Oberhagemann, *J. Am. Chem. Soc.* **2000**, *122*, 9237–9242.
- [22] B. Zibrowius, J. Caro, J. Kärger, *Z. Phys. Chem.* **1988**, *269*, 1101–1106.
- [23] J. Kärger, H. Pfeifer, W. Heink, *Adv. Magn. Opt. Reson.* **1988**, *12*, 1–89.
- [24] C. Chmelik, J. Kärger, *Chem. Soc. Rev.* **2010**, *39*, 4864–4884.
- [25] J. Kornatowski, *Zeolites* **1988**, *8*, 77–78.
- [26] S. Furukawa, C. McCabe, T. Nitta, P. T. Cummings, *Fluid Phase Equilib.* **2002**, *194–197*, 309–317.
- [27] M. Fernandez, J. Kärger, D. Freude, *Microporous Mesoporous Mater.* **2007**, *105*, 124–131.
- [28] K. Banas, F. Brandani, D. M. Ruthven, F. Stallmach, J. Kärger, *Magn. Reson. Imaging* **2005**, *23*, 227–232.
- [29] E. Beerdson, D. Dubbeldam, B. Smit, *J. Phys. Chem. B.* **2006**, *110*, 22754–22772.
- [30] R. Krishna, J. M. van Baten, *Microporous Mesoporous Mater.* **2011**, *137*, 83–91.
- [31] S. Y. Bhide, S. Yashonath, *J. Chem. Phys.* **1999**, *111*, 1658–1667.
- [32] T. J. H. Vlught, W. Zhu, F. Kapteijn, J. A. Moulijn, B. Smit, R. Krishna, *J. Am. Chem. Soc.* **1998**, *120*, 5599–5600.
- [33] J. Kärger, H. Pfeifer, F. Stallmach, N. N. Feoktistova, S. P. Zhdanov, *Zeolites* **1993**, *13*, 50–55.
- [34] J. Kärger, *Mol. Sieves* **2008**, *7*, 85–133.
- [35] J. Kärger, *J. Phys. Chem.* **1991**, *95*, 5558–5560.
- [36] S. Jost, N. K. Bär, S. Fritzsche, R. Haberlandt, J. Kärger, *J. Phys. Chem. B.* **1998**, *102*, 6375–6381.
- [37] P. Kortunov, S. Vasenkov, J. Kärger, R. Valiullin, P. Gottschalk, M. Fé Elía, M. Perez, M. Stöcker, B. Drescher, G. McElhiney, C. Berger, R. Gläser, J. Weitkamp, *J. Am. Chem. Soc.* **2005**, *127*, 13055–13059.
- [38] Y. Ma, D. Cai, Y. Li, N. Wang, U. Muhammad, A. Carlsson, D. Tang, W. Qian, Y. Wang, D. Su, F. Wei, *RSC Adv.* **2016**, *6*, 74797–74801.
- [39] J. Kärger, *ChemPhysChem* **2015**, *16*, 24–51.
- [40] J. Kärger, R. Valiullin, *Chem. Soc. Rev.* **2013**, *42*, 4172–4197.
- [41] R. Cotts, M. Hoch, T. Sun, J. Markert, *J. Magn. Reson.* **1989**, *83*, 252–266.

- [1] J. J. Li, M. Liu, X. W. Guo, C. Y. Dai, Z. M. Liu, C. S. Song, *Ind. Eng. Chem. Res.* **2018**, *57*, 8190–8199.
- [2] S. R. Zheng, A. Jentys, J. A. Lercher, *J. Catal.* **2006**, *241*, 304–311.
- [3] D. Ma, Y. Y. Shu, X. H. Bao, *J. Catal.* **2000**, *189*, 314–325.

Manuscript received: September 5, 2019  
 Revised manuscript received: October 12, 2019  
 Accepted manuscript online: October 29, 2019  
 Version of record online: December 5, 2019